A Spatial Model of Honey Bee Colony Collapse Due to Pesticide Contamination of Foraging Bees

P. Magal · G.F. Webb · Y. Wu.

Abstract We develop a model of honey bee colony collapse based on contamination of forager bees in pesticide contaminated spatial environments. The model consists of differential and difference equations for the spatial distributions of the uncontaminated and contaminated forager bees. A key feature of the model is incorporation of the return to the hive each day of forager bees. The model quantifies colony collapse in terms of two significant properties of honey bee colonies: (1) the fraction of contaminated forager bees that fail to return home due to pesticide contamination, and (2) the fraction of forager bees in the total forager bee population that return to the sites visited on the previous day. If the fraction of contaminated foragers failing to return home is high, then the total population falls below a critical threshold and colony collapse ensues. If the fraction of all foragers that return to previous foraging sites is high, then foragers who visit contaminated sites multiple times have a higher probability of becoming contaminated, and colony collapse ensues. This quantification of colony collapse provides guidance for implementing measures for its avoidance.

P. Magal
Université de Bordeaux, Bordeaux, France
Tel.: 33-40 00 21 10
E-mail: pierre.magal@u-bordeaux.fr

G.F. Webb
Vanderbilt University, Nashville, TN, USA
Tel.: 1-615-322-6661
E-mail: glenn.f.webb@vanderbilt.edu

Yixiang Wu
Vanderbilt University, Nashville, TN, USA
Tel.: 1-615-322-3659
E-mail: yixiang.wu@vanderbilt.edu

Mathematics Subject Classification (2010) 92D25 · 92D40
 whenever available.

1 Introduction

The connection of environmental pesticide contamination (EPC) to honey bee colony collapse disorder (CCD) is controversial. Many scientific studies have yielded conflicting reports, both supporting ([9], [24], [24], [32], [33]) and not supporting ([12], [13], [14], [15], [21], [49], [51], [56], [57], [59], [60]) a cause-effect connection. One class of pesticides, neuro-active neonicotinoids, has been identified as harmful, although sublethal, to honey bee colonies, particularly managed colonies in contaminated agricultural fields ([9], [20], [32], [33], [59], [60]). In an earlier work [48], we surveyed these studies, and developed a mathematical model to better understand this controversy. This model was based on a scalar difference equation formulation of honey bee colony population dynamics that incorporated the rate of homing failure of contaminated forager bees. This rate, together with the fractions of uncontaminated and contaminated forager bees, was critical in causation of CCD.

 Forager bees leave the hive at sunrise each day to gather pollen, resin, and other resources for the worker and juvenile bees in the hive ([1]). At sunset they return to the hive, and contribute to the care and rearing of juvenile bees ([1], [34], [42]). In [48] these issues were surveyed and incorporated into a model of CCD. In [48], a critical viability threshold of the forager population was analyzed, and proved deterministic for colony survival. If the sum of both uncontaminated and contaminated foragers was above this threshold, then CCD did not occur. Since contaminated forager bees had an increased homing failure above the normal homing failure of uncontaminated forager bees, the total forager population could be above or below the viability threshold. Thus, the total number of forager bees, as well as the fraction of contaminated forager bees, are deterministic for CCD. In [48], the fraction of contaminated bees that failed to return home each day and the daily rate of contamination were incorporated into a quantity R_1, which could predict CCD ($R_1 > 1$). Field studies specifying the value of R_1 could thus provide predictions for CCD.

 In this work, we extend the analysis in [48] to consider another significant factor of EPC in CCD: the spatial heterogeneity of contamination locations and the variability of forager bees in their patterns of returning to preferred location sites. Spatial heterogeneity of forager bees influences their survivability beyond the parametrically determined threshold in the spatially inhomogeneous case in [48]. The survivability threshold depends, in fact, on the spatial variation of contaminated regions. There are two main strategies that forager bees use to seek resources in their spatial environment: one is the use of social information from other bees communicated through waggle dancing to determine the distance and direction of preferred locations ([8], [41], [54], [55]); the other is the use of memorized information to fly to familiar preferred locations ([29], [30]). In 1973, Karl von Frisch won the Nobel Prize for his experiments

that established the role of waggle dancing in the communication of forager bees for preferred locations ([65]). However, recent experiments ([30]) found that 93% of the forager bees follow individually acquired information to locate resources.

In our model, we will assume that honey bee colonies are located in environments with an equal food resource gradient in all directions, where the social information communicated by waggle dancing is of less importance. We will assume that a proportion q of forager bees memorize the spatial information of their previous preferred locations, and go repeatedly to these locations. The remaining $1-q$ proportion of bees, travel in random directions to seek new resources. Thus, heterogeneous spatial pesticide contamination in the colony foraging region results in variable fractions of the forager bee population that become contaminated. Our model is designed, particularly, for application to managed colonies in industrial agricultural settings, where these spatial conditions are common.

The organization of this paper is as follows: in Section 2 we formulate our spatial model of the population dynamics of forager bees; in Section 3 we analyze our model without pesticide contamination in the spatial environment; in Section 4 we analyze our model with pesticide contamination in the spatial environment; in Section 5 we provide numerical simulations of our model; and in Section 6 we provide some conclusions from our model for EPC in CCD.

2 Spatial distribution of forager bees

In this section, we formulate a model for the spatial distribution of forager bees. In our model, we do not include worker bees in the hive, who are a majority of the bee population, with primary function to care for juvenile bees. Worker bees remain in the hive and do not become contaminated from contact with pesticides outside the hive. We define $\mathcal{G}(\tau, x, y)$, $(x, y) \in \mathbb{R}_+^2$, as the spatial probability density function of forager bees in the hive, where τ is a given value. Thus, $\mathcal{G}(\tau, x, y)$ satisfies

$$\iint_{\mathbb{R}^2} \mathcal{G}(\tau, x, y) \, dx \, dy = 1, \text{ for } \tau > 0.$$

For simplicity, we choose $\mathcal{G}$ as the Gaussian function

$$\mathcal{G}(\tau, x, y) = \frac{1}{4\pi\epsilon\tau} e^{-\frac{(x-x_0)^2 + (y-y_0)^2}{4\epsilon\tau}},$$

where (x_0, y_0) is center of the hive and $\sigma = \sqrt{2\epsilon\tau}$ is the standard deviation of $\mathcal{G}$ for a given value of ϵ and τ. The choice of a Gaussian distribution is made for simplicity, since the hive is very small in relation to the foraging region. The values of ϵ and τ are chosen so that $\mathcal{G}$ represents a very small region compared to the foraging region of forager bees. The foraging region is taken

as all of $\mathbb{R}^2$, where it is understood that forager bees remain near the hive and away from the boundaries of the foraging region, as governed by the spatial parameters of the model.

Let $\Delta = \frac{\partial^2}{\partial x^2} + \frac{\partial^2}{\partial y^2}$ be the Laplacian in $L^1(\mathbb{R}^2)$ and let $\{T(t)\}_{t \geqslant 0}$ be the strongly continuous semigroup of bounded linear operators in $L^1(\mathbb{R}^2)$ generated by $\epsilon \Delta$:

$$(T(t)g)(x,y) = \frac{1}{4\pi\epsilon t} \iint_{\mathbb{R}^2} e^{-\frac{(x-\widehat{x})^2+(y-\widehat{y})^2}{4\epsilon t}} g(\widehat{x}, \widehat{y}) \, d\widehat{x} \, d\widehat{y}, \ \ \text{for } g \in L^1(\mathbb{R}^2), \ t \geqslant 0.$$

Then, $\mathcal{G}(\tau, x, y) = (T(\tau)\delta)(x,y)$, where δ is the Dirac delta function centered at (x_0, y_0). By the semigroup property of $\{T(t)\}_{t \geqslant 0}$, we have

$$(T(t+\tau)\delta)(x,y) = (T(t)T(\tau)\delta)(x,y) = \mathcal{G}(t+\tau, x, y), \ t, \tau \geqslant 0, \ (x,y) \in \mathbb{R}^2,$$

where $\mathcal{G}(\tau + t, x, y)$ is the spatial distribution of forager bees at time t with respect to spatial location $(x,y) \in \mathbb{R}^2$ in the environmental region of the colony.

3 Model without pesticide contamination

We first assume that there is no pesticide contamination in the environment. Forager bees leave the hive at sunrise each day and return to the hive at nightfall. Let $u(t, x, y)$ be the density of forager bees at time t and location $(x, y) \in \mathbb{R}^2$. At the start of the first day, the initial distribution of forager bees is

$$u(0, x, y) = u_0(x, y) \geqslant 0,$$

where $u_0 \in L^1_+(\mathbb{R}^2)$, and

$$U_0 = \iint_{\mathbb{R}^2} u_0(x, y) dx dy$$

is the total number of forager bees at time $t = 0$.

During the first day, the forager bees diffuse randomly in $\mathbb{R}^2$, which means that u satisfies the following equation for each $t \in [0, 1)$:

$$\partial_t u(t, x, y) = \varepsilon \Delta u(t, x, y) - \mu(x, y) u(t, x, y), \ \text{for } (x, y) \in \mathbb{R}^2, \qquad (1)$$

where

$$U(t) = \iint_{\mathbb{R}^2} u(t, x, y) \, dx \, dy,$$

is the total number of forager bees at time $t \in [0, 1)$, $\mu(x, y) \geqslant 0$ is the mortality rate of the bees, and ε is the diffusion rate. The mortality rate $\mu(x, y)$ incorporates homing failure and all other causes of mortality for forager bees. We assume that μ is a bounded continuous nonnegative function on $\mathbb{R}^2$.

At the end of the first day, we assume that all forager bees not subject to mortality return home, and the total population at the end of the first day is

$$U(1^-) = \iint_{\mathbb{R}^2} u(1^-, x, y) \, dx \, dy.$$

The forager bees that have returned to the hive on the first day contribute to the care of juvenile bees in the hive. We use the following Allee functional to describe their contribution to the production of forager bees that eventually leave the hive to go foraging:

$$\frac{\beta \, U(1^-)^2}{\chi^2 + U(1^-)^2},$$

where β is the maximal production parameter and χ is the sigmoidal Hill function production parameter ([48]).

Remark 1 Many mathematical models of CCD have used Allee forms involving the development of juvenile bees, including [2], [3], [4], [5], [10], [11], [18], [19], [26], [27], [36], [37], [39], [40], [43], [47], [52], [53], [64].

There are two types of behaviors of forager bees, when they return home at the end of the day and go foraging the next day. A proportion of forager bees will return back to the hive and start over the next day from the hive without memory of their location the previous day. We model their foraging behavior on the second day with diffusion. The second type of behavior of forager bees involves those who remember a favorable foraging location from the previous day. In the morning of the next day, these bees will go directly to these locations.

By combining these two types of behavior and supposing that the forager bees distribute in the hive following the Gaussian probability density $\mathcal{G}(\tau, x, y)$, we obtain $u_1(x, y)$, which is the distribution of forager bees in the morning of the second day:

$$u_1(x, y) = \mathcal{G}(\tau, x, y) \left(\frac{\beta \, U(1^-)^2}{\chi^2 + U(1^-)^2} + (1 - q) \, U(1^-) \right) + qu(1^-, x, y), \quad (2)$$

where $q \in [0, 1]$ is the fraction of forager bees that follow the second type of behavior.

In (2), $\mathcal{G}(\tau, x, y) \left(\frac{\beta \, U(1^-)^2}{\chi^2 + U(1^-)^2} \right)$ represents the new forager bees produced in the hive. The term $\mathcal{G}(\tau, x, y)(1 - q) \, U(1^-)$ represents the bees that start the second day by diffusing from the hive. The term $qu(1^-, x, y)$ represents the bees that remember their locations from the previous day and start the next day from these locations. We neglect the time required for their travel to these locations, which is very short.

Remark 2 We remark that environmental resource heterogeneity could be incorporated by assuming that the fraction $q = q(x, y)$ is spatially dependent. Field studies have shown that bees are more likely to return back to resource favorable locations ([38], [50], [61]).

3.1 Case $q = 0$ and $\mu(x, y)$ constant

When $q = 0$ all the bees we will diffuse from the hive in the morning of the next day. In this case we obtain

$$u_1(x, y) = \mathcal{G}(\tau, x, y) \left(\frac{\beta \, U(1^-)^2}{\chi^2 + U(1^-)^2} + U(1^-) \right).$$

The dynamical properties of the model in this case are similar to the spatially independent model without space in [48].

Suppose that μ is a constant. Since $q = 0$, without loss of generality, we assume that $u_0(x, y)$ is a multiple of $\mathcal{G}(\tau, x, y)$. Then, in the morning of the first day, the initial condition is

$$u_0(x, y) = \mathcal{G}(\tau, x, y) U(0) = U(0)(T(\tau)\delta)(x, y).$$

By (1), we have

$$u(t, \cdot, \cdot) = e^{-\mu t} T(t) u_0 = U(0) e^{-\mu t} T(t + \tau)\delta, \quad t \in (0, 1),$$

and at sunset of the first day, the population density is

$$u(1^-, \cdot, \cdot) = e^{-\mu} T(1) u_0 = e^{-\mu} U(0) T(1 + \tau)\delta.$$

Thus, the total population at sunset of the first day is

$$U(1^-) = \iint_{\mathbb{R}^2} u(1^-, x, y) \, dx \, dy = e^{-\mu} U(0).$$

Taking into consideration the recruitment of new forager bees, the population at the sunrise of the second day is

$$\begin{aligned} u(1, x, y) &= \mathcal{G}(\tau, x, y) U(1) \\ &= \mathcal{G}(\tau, x, y) \left(\frac{\beta \, U(1^-)^2}{\chi^2 + U(1^-)^2} + U(1^-) \right) \\ &= \mathcal{G}(\tau, x, y) \left(\frac{\beta \, (e^{-\mu} U(0))^2}{\chi^2 + (e^{-\mu} U(0))^2} + e^{-\mu} U(0) \right) \\ &= \mathcal{G}(\tau, x, y) \left(\frac{\beta \, U(0)^2}{\widetilde{\chi}^2 + U(0)^2} + e^{-\mu} U(0) \right) \end{aligned}$$

where

$$\widetilde{\chi} := \frac{\chi}{e^{-\mu}}.$$

For days $n = 1, 2, \ldots$, we obtain the difference equation

$$u(n + 1, x, y) = \mathcal{G}(\tau, x, y) \left(\frac{\beta \, U(n)^2}{\widetilde{\chi}^2 + U(n)^2} + e^{-\mu} U(n) \right). \tag{3}$$

Therefore, integrating over $\mathbb{R}^2$, we obtain the difference equation

$$U(n+1) = \frac{\beta\, U(n)^2}{\widetilde{\chi}^2 + U(n)^2} + e^{-\mu}U(n),\ n = 0, 1, \dots. \tag{4}$$

Define

$$\widetilde{\beta} := \frac{\beta}{1 - e^{-\mu}},$$

and

$$R_0 := \frac{\widetilde{\beta}}{2\widetilde{\chi}} = \frac{\beta e^{-\mu}}{2\chi\,(1 - e^{-\mu})}.$$

The equilibria for (4) are

$$0 < \overline{U}_- := \frac{\widetilde{\beta} - \sqrt{\widetilde{\beta}^2 - 4\widetilde{\chi}^2}}{2} < \overline{U}_+ := \frac{\widetilde{\beta} + \sqrt{\widetilde{\beta}^2 - 4\widetilde{\chi}^2}}{2},$$

whereever $R_0 > 1$. When $R_0 < 1$, (4) has only trivial equilibrium 0.

Remark 3 If $\overline{U}_-$, $\overline{U}_+$, and μ are known, then β and χ can be determined by the following formulas:

$$\widetilde{\beta} = \overline{U}_+ + \overline{U}_- = \frac{\beta}{1 - e^{-\mu}},$$

$$\widetilde{\chi}^2 = \frac{(\overline{U}_+ + \overline{U}_-)^2 - (\overline{U}_+ - \overline{U}_-)^2}{4} = \chi^2 e^{2\mu}.$$

Theorem 1 *Suppose $q = 0$ and μ is constant. The following hold:*

(i) *If $R_0 < 1$, the only equilibrium of (3) in $L^1(\mathbb{R}^2)$ is 0, which is globally asymptotically stable.*

(ii) *If $R_0 > 1$, (3) has three nonnegative equilibria in $L^1(\mathbb{R}^2)$: $0, \overline{u}_-, \overline{u}_+$, where*

$$0 < \overline{u}_- = \mathcal{G}(\tau, x, y)\overline{U}_- < \overline{u}_+ := \mathcal{G}(\tau, x, y)\overline{U}_+.$$

Moreover, 0 and $\overline{u}_+$ are locally asymptotically stable. If $U(0) \in [0, \overline{U}_-)$, the solution converges to 0; if $U(0) \in (\overline{U}_-, \infty)$, the solution converges to $\overline{u}_+$.

Proof In Lemma 2.1 in ([48]), we proved that if $R_0 < 1$, then $U(n)$ converges to 0, and if $R_0 > 1$, then $U(n)$ converges to 0 when $U(0) \in (0, \overline{U}_-)$, and $U(n)$ converges to $\overline{U}_+$ when $U(0) \in (\overline{U}_-, \infty)$. Define $\overline{u}(x, y) := \mathcal{G}(\tau, x, y)\overline{U}$, where $\overline{U} = 0, \overline{U}_-$, or $\overline{U}_+$. Then,

$$\iint\limits_{\mathbb{R}^2} |u(n, x, y) - \overline{u}(x, y)|\, dx\, dy = \iint\limits_{\mathbb{R}^2} |\mathcal{G}(\tau, x, y)U(n) - \overline{u}(x, y)|\, dx\, dy$$

$$= |U(n) - \overline{U}|,$$

and the conclusions follow from Lemma 2.1 in [48].

3.2 Case $q \geqslant 0$ and $\mu(x, y)$ is not constant

We impose the following additional assumption on $\mu(x, y)$: There exists a constant $\mu_0 > 0$ such that

$$\mu(x, y) \geqslant \mu_0, \text{ for all } (x, y) \in \mathbb{R}^2. \tag{5}$$

We work in the complete metric space $X = L_+^1(\mathbb{R}^2)$ with the metric induced by the L^1 norm. Let $L : L_+^1(\mathbb{R}^2) \to L_+^1(\mathbb{R}^2)$ be the operator defined by

$$L(u_0) = u_1,$$

where u_1 is defined in (2) and $u_0 \in L_+^1(\mathbb{R}^2)$.

In order to describe the long term behavior of the model, we consider the following spatial difference equation

$$\begin{cases} u_{n+1} = L u_n, \, n = 0, 1, \ldots, \\ u_0 \in L_+^1(\mathbb{R}^2). \end{cases} \tag{6}$$

We will prove the existence of a global attractor of L. Let $\boldsymbol{\alpha}$ be the Kuratowski measure of noncompactness, i.e.

$$\boldsymbol{\alpha}(B) = \inf\{r > 0 : B \text{ has a finite cover of sets of diameter less than } r\},$$

for any bounded set $B \subset X$.

We recall definitions and results concerning global attractors (see Chapter 2 in [31] or Chapter 1 in [66]). A continuous mapping F on a complete metric space (Z, d) is said to be *point dissipative* if there exists a bounded set $B \subset Z$ such that $L^n u_0 \in B$ for all $u_0 \in Z$ and $n \geqslant N = N(u_0)$; F is said to be $\boldsymbol{\alpha}$-*condensing* if $\boldsymbol{\alpha}(L(B)) < \boldsymbol{\alpha}(B)$ for any nonempty bounded closed set $B \subset Z$ with $\boldsymbol{\alpha}(B) > 0$, and F maps bounded sets into bounded sets in Z; a connected, compact, invariant (that is, $F(A) = A$) set $A \subset Z$ is said to be a *global attractor* for F if A attracts bounded sets of Z in the sense that

$$\lim_{n \to \infty} \delta\left(F^n(B), A\right) = 0$$

where Hausdorff semi-distance $\delta\left(B, A\right)$ is defined by

$$\delta\left(B, A\right) = \sup_{u \in B} \inf_{v \in A} d(u, v).$$

If F is point dissipative, $\boldsymbol{\alpha}$-condensing, and orbits of bounded sets are bounded, then F has a global attractor.

Theorem 2 (Existence of global attractor) *Suppose (5) holds. Let the mapping $L : X \to X$ be defined as above. Then, L is monotone increasing, point dissipative, and $\boldsymbol{\alpha}$-condensing. Moreover, L has a global attractor.*

Proof The monotonicity of L follows from the comparison principle of parabolic problems and the monotonicity of (2). First, we show that L is point dissipative. For any $u_0 \in X$, by the variation of constant formula, for $t \in (0, 1)$, we have

$$u(t, \cdot, \cdot) = e^{-\mu_0 t} T(t) u_0 - \int_0^t e^{-\mu_0(t-s)} T(t-s)(\mu - \mu_0) u(s, \cdot, \cdot) ds,$$
$$\leqslant e^{-\mu_0 t} T(t) u_0.$$

Therefore,

$$U(1^-) \leqslant e^{-\mu_0} U(0).$$

It follows that

$$\|u_1\|_{L^1} = \iint_{\mathbb{R}^2} \left(\mathcal{G}(\tau, x, y) \left(\frac{\beta U(1^-)^2}{\chi^2 + U(1^-)^2} + (1-q) U(1^-) \right) + qu(1^-, x, y) \right) dx dy$$

$$= \frac{\beta U(1^-)^2}{\chi^2 + U(1^-)^2} + U(1^-)$$

$$\leqslant \frac{\beta U(0)^2}{\widetilde{\chi}^2 + U(0)^2} + e^{-\mu_0} U(0)$$

$$= \frac{\beta \|u_0\|_{L^1}^2}{\widetilde{\chi}^2 + \|u_0\|_{L^1}^2} + e^{-\mu_0} \|u_0\|_{L^1}.$$

Therefore,

$$\|Lu_0\|_{L^1} \leqslant \frac{\beta \|u_0\|_{L^1}^2}{\widetilde{\chi}^2 + \|u_0\|_{L^1}^2} + e^{-\mu_0} \|u_0\|_{L^1}. \tag{7}$$

Since $\|Lu_0\|_{L^1} \leqslant \beta + e^{-\mu_0} \|u_0\|_{L^1}$, we have

$$\|L^n u_0\|_{L^1} \leqslant \beta + e^{-\mu_0}(\beta + e^{-\mu_0} \|L^{n-2} u_0\|_{L^1})$$
$$= \beta + \beta e^{-\mu_0} + e^{-2\mu_0} \|L^{n-2} u_0\|_{L^1}.$$

By induction,

$$\|L^n u_0\|_{L^1} \leqslant \sum_{k=0}^{n-1} \beta e^{-k\mu_0} + e^{-n\mu_0} \|u_0\|_{L^1}$$

$$\leqslant \frac{\beta}{1 - e^{-\mu_0}} + e^{-n\mu_0} \|u_0\|_{L^1}.$$

Therefore, L is point dissipative, and the orbits of bounded sets of L are bounded, that is, for any bounded set $B \subset X$, the set $\{L^n u_0 : n \geqslant 0 \text{ and } u_0 \in B\}$ is bounded in X.

We show that L is $\boldsymbol{\alpha}$-condensing. From (7), we can see that L maps bounded sets to bounded sets in X. The mapping L can be decomposed as $L = L_1 + L_2$, where

$$L_1 u_0 = \mathcal{G}(\tau, x, y) \left(\frac{\beta U(1^-)^2}{\chi + U(1^-)^2} + (1-q) U(1^-) \right)$$

and
$$L_2 u_0 = q u(1^-, x, y).$$
where $u(1^-, x, y)$ is the solution of (1) at time $t = 1$.

Since L_1 is of rank 1, it is compact. Since $\|L_2 u_0\|_{L^1} \leqslant q e^{-\mu_0}\|u_0\|_{L^1}$, for any bounded set $B \subset X$, we have

$$\boldsymbol{\alpha}(L(B)) \leqslant \boldsymbol{\alpha}(L_1(B)) + \boldsymbol{\alpha}(L_2(B)) = \boldsymbol{\alpha}(L_2(B)) \leqslant q e^{-\mu_0}\boldsymbol{\alpha}(B).$$

Therefore, L is $\boldsymbol{\alpha}$-condensing. Since L is point dissipative, $\boldsymbol{\alpha}$-condensing, and the orbits of bounded sets of L are bounded, L has a global attractor.

3.3 Case $q > 0$ and $\mu(x, y)$ constant

We note that R_0 does not depend on q. When $\mu(x, y)$ is constant and $q > 0$, the solution of (6) satisfies the following difference equation:

$$u_{n+1}(x, y) = \mathcal{G}(\tau, x, y) h\left(U(n)\right) + q e^{-\mu}(T(1)u_n)(x, y), \qquad (8)$$

where

$$h(U) := \frac{\beta\, U^2}{\widetilde{\chi}^2 + U^2} + (1 - q)e^{-\mu}U,$$

and

$$U(n) = \iint\limits_{\mathbb{R}^2} u_n(x, y)\, dx\, dy.$$

By integration of (8) in space, we obtain (4). So the dynamics of the total population is described by (4).

Equilibria: The equilibrium solution satisfies

$$\bar{u} = \mathcal{G}(\tau, x, y)\left(\frac{\beta\, \bar{U}^2}{\widetilde{\chi}^2 + \bar{U}^2} + (1 - q)\, e^{-\mu}\bar{U}\right) + q e^{-\mu}T(1)\bar{u},$$

where

$$\bar{U} = \iint\limits_{\mathbb{R}^2} \bar{u}(x, y)\, dx\, dy.$$

By integrating in space, we obtain the equilibrium equation for (4). Therefore, $\bar{U}$ is equal to $0, \bar{U}_-$ or $\bar{U}_+$. Define

$$U^\star := \frac{\beta\, \bar{U}^2}{\widetilde{\chi}^2 + \bar{U}^2} + (1 - q)\, e^{-\mu}\bar{U},$$

then

$$\begin{aligned}
\bar{u} &= \mathcal{G}(\tau, x, y)U^\star + q e^{-\mu}T(1)\left(\mathcal{G}(\tau, x, y)U^\star + q e^{-\mu}T(1)(\bar{u})\right)\\
&= \mathcal{G}(\tau, x, y)U^\star + q e^{-\mu}\mathcal{G}(\tau + 1, x, y)U^\star + \left(q e^{-\mu}\right)^2 T(2)\left(\bar{u}\right)
\end{aligned}$$

and, by induction, we obtain

$$\bar{u} = \Sigma_{n \geqslant 0}\left(q e^{-\mu}\right)^n \mathcal{G}(\tau + n, x, y)U^\star. \qquad (9)$$

By integrating both side of (9), we deduce that

$$\overline{U} = \sum_{n \geqslant 0} (qe^{-\mu})^n U^\star = \frac{1}{1 - qe^{-\mu}} U^\star,$$

which implies

$$U^\star = \left(1 - qe^{-\mu}\right) \overline{U}.$$

Therefore, replacing $U^\star$ in (9), we obtain an explicit formula for the equilibrium

$$\overline{u} = \left(1 - qe^{-\mu}\right) \Sigma_{n \geqslant 0} \left(qe^{-\mu}\right)^n \mathcal{G}(\tau + n, x, y)\overline{U}. \tag{10}$$

Theorem 3 *Suppose that μ is constant. Let $\{u_n\}$ be the solution of (6). The following results hold:*

(i) *If $R_0 < 1$, then u_n converges to $0 \in L^1$.*
(ii) *If $R_0 > 1$ we have the following alternatives:*
    (a) *If $U(0) < \overline{U}_-$ then $\lim_{n \to \infty} u_n = 0$ in L^1;*
    (b) *If $U(0) = \overline{U}_-$ then $\lim_{n \to \infty} u_n = \overline{u}_-$ in L^1;*
    (c) *If $U(0) > \overline{U}_-$ then $\lim_{n \to \infty} u_n = \overline{u}_+$ in L^1.*

Proof (i): If $R_0 < 1$, by ref[Lemma 2.1, MWW], we have $\lim_{n \to \infty} U(n) = 0$. Therefore, $\lim_{n \to \infty} L^n u_0 = 0$ in $L^1(\Omega)$.
(ii): Since the total population satisfies (4), by Lemma 2.1 in [48] we have $\lim_{n \to \infty} U(n) = \overline{U}$ where $\overline{U} = 0$ if $U(0) < \overline{U}_-$, $\overline{U} = \overline{U}_-$ if $U(0) = \overline{U}_-$, and $\overline{U} = \overline{U}_+$ if $U(0) > \overline{U}_-$.

By Theorem 2, we know that $\{u_n\}_{n \geqslant 0}$ is relatively compact. Therefore, there exists an omega-limit set $\omega(u_0)$ which is invariant by L. Let $\{v_n\}_{n \in \mathbb{Z}}$ by a complete orbit of (8) on $\omega(u_0)$. Then for each $n \in \mathbb{Z}$

$$v_{n+1}(x, y) = \mathcal{G}(\tau, x, y)h\left(\overline{U}\right) + qe^{-\mu}(T(1)v_n)(x, y).$$

Therefore

$$v_{n+1}(x, y) = \mathcal{G}(\tau, x, y)h\left(\overline{U}\right) + qe^{-\mu}(T(1)\mathcal{G}(\tau, x, y)h\left(\overline{U}\right))(x, y)$$

$$+ \left(qe^{-\mu}\right)^2 (T(2)v_{n-1})(x, y),$$

and by induction we obtain for each integer $n \in \mathbb{Z}$

$$v_n = \Sigma_{k \geqslant 0} \left(qe^{-\mu}\right)^n \mathcal{G}(\tau + n, x, y)\overline{U} = \overline{u}.$$

Therefore, $\omega(u_0) = \{\overline{u}\}$ and the proof is complete.

4 Model with pesticide contamination

In this section, we will model the effect of contamination due to pesticide in the environment on the dynamics of forager bees. Let $u(t, x, y)$ and $c(t, x, y)$ be the density of uncontaminated and contaminated forager bees at time t and location $(x, y) \in \mathbb{R}^2$, respectively. We start day one with the initial distribution

$$u(0, x, y) = u_0(x, y) \text{ and } c(0, x, y) = c_0(x, y),$$

where $u_0, c_0 \in L^1_+(\mathbb{R}^2)$.

During the first day, the spatial dynamics of the forager bee population is described for $t \in [0, 1)$ by

$$\begin{cases} \partial_t u(t, x, y) = \varepsilon \Delta u(t, x, y) - \mu(x, y) u(t, x, y) - \alpha(x, y) u(t, x, y) \\ \partial_t c(t, x, y) = \varepsilon \Delta c(t, x, y) - \mu(x, y) c(t, x, y) + \alpha(x, y) u(t, x, y) \end{cases} \quad (11)$$

where $\varepsilon > 0$ is the diffusion rate, $\mu(x, y)$ is the mortality rate of the bees and $\alpha(x, y)$ is the rate of contamination of the forager bees by pesticides. We assume that α and μ are bounded continuous nonnegative functions on $\mathbb{R}^2$.

At the end of the day, the number of uncontaminated and contaminated bees are respectively

$$U(1^-) = \iint\limits_{\mathbb{R}^2} u(1^-, x, y) dx dy \text{ and } C(1^-) = \iint\limits_{\mathbb{R}^2} c(1^-, x, y) dx dy.$$

We assume that a fraction $1 - p$ of contaminated forager bees fail to return home at the end of each day, in addition to the normal homing failure of all foraging bees contained in the mortality rate μ. Then by combining the previous mechanisms, we obtain the following model

$$u_1(x, y) = \mathcal{G}(\tau, x, y) \left[B + (1 - q) U(1^-) \right] + q u(1^-, x, y) \quad (12)$$

$$c_1(x, y) = \mathcal{G}(\tau, x, y) \left[(1 - q) p C(1^-) \right] + q p c(1^-, x, y) \quad (13)$$

where

$$B = \frac{\beta \left(U(1^-) + pC(1^-) \right)^2}{\chi^2 + \left(U(1^-) + pC(1^-) \right)^2}. \quad (14)$$

On the second day, we replace the initial values $u(0, x, y) = u_0(x, y)$ and $c(0, x, y) = c_0(x, y)$ by $u(1, x, y) = u_1(x, y)$ and $c(1, x, y) = c_1(x, y)$, and we solve (11) with this new initial condition on the time interval $t \in [1, 2]$. The same process carries over to time intervals $[2, 3], [3, 4]$ and so on.

Remark 4 Our formulation of the increased homing failure of contaminated bees, beyond the normal homing failure in the mortality rate $\mu(x, y)$, as an increased homing failure fraction $1 - p$, relates to field studies ([3], [32], [33]). In these studies, individual bees were monitored with radio-frequency tags, which provided specific identification of homing failure as the cause of mortality. It

is recognized that pesticide contamination has sublethal effect on forager bees ([3], [11], [20], [21], [44], [58], [59]). The connection of EPC to CCD is indirect in that forager bees have reduced days for foraging and reduced contributions to caring for juvenile bees in the hive, but are not directly lethally affected.

Let $Y = L^1_+(\Omega) \times L^1_+(\Omega)$ with the metric induced by the $L^1 \times L^1$ norm. Let $S : Y \to Y$ be a continuous mapping defined by

$$S(u_0, c_0) = (u_1, c_1), \ (u_0, c_0) \in Y.$$

To study the dynamics of this model, we need to consider the solutions of the following spatial difference equation:

$$\begin{cases} (u_{n+1}, c_{n+1}) = S(u_n, c_n), \ n = 0, 1, \ldots, \\ (u_0, c_0) \in Y. \end{cases} \tag{15}$$

4.1 Case q=0, $\mu(x, y)$ and $\alpha(x, y)$ constant

Since $q = 0$, we may also assume that u_0 and c_0 are multiples of $\mathcal{G}(\tau, x, y)$:

$$u_0(x, y) = U(0)\mathcal{G}(\tau, x, y) = U(0)(T(\tau)\delta)(x, y),$$

$$c_0(x, y) = C(0)\mathcal{G}(\tau, x, y) = C(0)(T(\tau)\delta)(x, y).$$

By the first equation of (11), we have

$$u(t, \cdot, \cdot) = e^{-(\mu+\alpha)t}T(t)u_0, \ t \in (0, 1).$$

Summing up the two equations of (11), we obtain

$$(u + c)(t, \cdot, \cdot) = e^{-\mu t}T(t)(u_0 + c_0), \ t \in (0, 1).$$

Therefore,

$$c(t, \cdot, \cdot) = e^{-\mu t}(1 - e^{-\alpha t})T(t)u_0 + e^{-\mu t}T(t)c_0, \ t \in (0, 1).$$

It follows that

$$U(1^-) = e^{-(\mu+\alpha)}U(0) \text{ and } C(1^-) = e^{-\mu}\left\{C(0) + \left[1 - e^{-\alpha}\right]U(0)\right\}.$$

By (12)-(14) and $q = 0$, for $n = 0, 1, \ldots$, we have

$$\begin{cases} u_{n+1}(x, y) = \mathcal{G}(\tau, x, y)\left[\dfrac{\beta V(n)^2}{\chi^2 + V(n)^2} + e^{-(\mu+\alpha)}U(n)\right] \\ c_{n+1}(x, y) = \mathcal{G}(\tau, x, y)[pe^{-\mu}C(n) + pe^{-\mu}\left[1 - e^{-\alpha}\right]U(n)] \end{cases} \tag{16}$$

with

$$V(n) := pe^{-\mu}C(n) + \left[pe^{-\mu} + (1-p)e^{-(\alpha+\mu)}\right]U(n).$$

Integrating over $\mathbb{R}^2$, we obtain

$$
\begin{cases}
U(n+1) = \dfrac{\beta\,V(n)^2}{\chi^2 + V(n)^2} + e^{-(\mu+\alpha)}U(n), \\[4mm]
C(n+1) = pe^{-\mu}C(n) + pe^{-\mu}\left[1 - e^{-\alpha}\right]U(n),
\end{cases} \tag{17}
$$

where the equations in (17) are the same as in the model without space ([48]). Define

$$
\widehat{\beta} := \frac{\beta}{1 - e^{-(\mu+\alpha)}} \quad \text{and} \quad \widehat{\chi} := \frac{\chi}{e^{-(\mu+\alpha)}\left[1 + p\kappa_2\right]}
$$

with

$$
\kappa_1 := \frac{p\,e^{-\mu}\left[1 - e^{-\alpha}\right]}{1 - p\,e^{-\mu}} \quad \text{and} \quad \kappa_2 := e^\alpha\left\{\kappa_1 + \left[1 - e^{-\alpha}\right]\right\} = \frac{e^\alpha - 1}{1 - pe^{-\mu}}.
$$

Let

$$
R_1 := \frac{\widehat{\beta}}{2\widehat{\chi}} = \frac{\beta\left[1 + p\kappa_2\right]}{2\chi\left[e^{(\mu+\alpha)} - 1\right]} = \frac{\beta\left[\left[1 - pe^{-\mu}\right] + p\left[e^\alpha - 1\right]\right]}{2\chi\left[e^{(\mu+\alpha)} - 1\right]\left[1 - pe^{-\mu}\right]}.
$$

The following result follows from the analysis in [48]:

Theorem 4 *Suppose that $q = 0$ and $\mu(x, y)$ and $\alpha(x, y)$ are constant functions. Let $\{(u_n(x, y), c_n(x, y))\}$ be the solution of (15). Then the following results hold:*

(i) *If $R_1 < 1$, then $\lim_{n\to\infty}(u_n, c_n) = (0, 0) \in L^1 \times L^1$ in Y.*
(ii) *If $R_1 > 1$, then (15) has three equilibria in Y:*

$$
(0, 0) \ll \mathcal{G}(\tau, x, y)(\overline{U}_-, \overline{C}_-) \ll \mathcal{G}(\tau, x, y)(\overline{U}_+, \overline{C}_+),
$$

where

$$
\overline{C}_\pm = \kappa_1 \overline{U}_\pm,
$$

and

$$
0 < \overline{U}_- := \frac{\widehat{\beta} - \sqrt{\widehat{\beta}^2 - 4\widehat{\chi}^2}}{2} < \overline{U}_+ := \frac{\widehat{\beta} + \sqrt{\widehat{\beta}^2 - 4\widehat{\chi}^2}}{2}.
$$

Moreover if $U_0 < \overline{U}_-$ and $C_0 < \overline{C}_-$, then $\lim_{n\to\infty}(u_n, c_n) = (0, 0)$ in Y; if $U_0 > \overline{U}_-$ and $C_0 > \overline{C}_-$, then $\lim_{n\to\infty}(u_n, c_n) = \mathcal{G}(\tau, x, y)(\overline{U}_+, \overline{C}_+)$ in Y.

Proof In [48, Lemma 3.1, Propositions 3.2-3.3], we have proved that the solution $(U(n), C(n))$ of (17) satisfies: if $R_1 < 1$, $(U(n), C(n))$ converges to $(0, 0)$; if $R_1 > 1$, $(U(n), C(n))$ converges to $(0, 0)$ when $U_0 < \overline{U}_-$ and $C_0 < \overline{C}_-$ and $(U(n), C(n))$ converges to $(\overline{U}_+, \overline{C}_+)$ when $U_0 > \overline{U}_-$ and $C_0 > \overline{C}_-$. The results then follow from (16).

4.2 Case $q \geqslant 0$

In this section we prove the existence of a global attractor for S, when $q \geqslant 0$.

Theorem 5 (Existence of global attractor) *Suppose (5) holds. Let the mapping $S : Y \to Y$ be defined as above. Then, S is point dissipative and $\boldsymbol{\alpha}$-condensing. Moreover, S has a global attractor.*

Proof First, we show S is point dissipative and maps bounded sets to bounded sets. From (5) $\mu(x, y) \geqslant \mu_0$, and by the first equation of (11), we have

$$u(t, \cdot, \cdot) = e^{-\mu_0 t} T(t) u_0 - \int_0^t e^{-\mu_0(t-s)} T(t-s)(\alpha + \mu - \mu_0) u(s, \cdot, \cdot) ds$$
$$\leqslant e^{-\mu_0 t} T(t) u_0,$$

for all $t \in (0, 1)$. Therefore,

$$U(t) \leqslant e^{-\mu_0 t} \|u_0\|_{L^1}, \ t \in (0, 1). \tag{18}$$

Summing the two equations in (11), we have

$$c(t, \cdot, \cdot) \leqslant u(t, \cdot, \cdot) + c(t, \cdot, \cdot)$$
$$= e^{-\mu_0 t} T(t)(u_0 + c_0) - \int_0^t e^{-\mu_0(t-s)} T(t-s)(\mu - \mu_0)(u(s, \cdot, \cdot)$$
$$+ c(s, \cdot, \cdot)) ds \tag{19}$$
$$\leqslant e^{-\mu_0 t} T(t)(u_0 + c_0),$$

for all $t \in (0, 1)$. Therefore, for all $t \in (0, 1)$, we have

$$C(t) \leqslant e^{-\mu_0 t}(\|u_0\|_{L^1} + \|c_0\|_{L^1}). \tag{20}$$

Combining (18)-(20), we have

$$\begin{cases} U(1^-) \leqslant e^{-\mu_0} \|u_0\|_{L^1}, \\ C(1^-) \leqslant e^{-\mu_0}(\|u_0\|_{L^1} + \|c_0\|_{L^1}). \end{cases} \tag{21}$$

By (12)-(13), we have

$$\begin{cases} \|u_1\|_{L^1} = \iint\limits_{\mathbb{R}^2} u_1(x, y) dx dy = \dfrac{\beta \ (U(1^-) + pC(1^-))^2}{\chi^2 + (U(1^-) + pC(1^-))^2} + U(1^-), \\ \|c_1\|_{L^1} = \iint\limits_{\mathbb{R}^2} c_1(x, y) dx dy = pC(1^-). \end{cases} \tag{22}$$

It follows that S maps bounded sets to bounded sets in Y. By the first equations of (21) and (22), $\|u_1\|_{L^1} \leqslant \beta + e^{-\mu_0} \|u_0\|_{L^1}$. Using an induction argument similar to the proof of Theorem 2, we obtain

$$\|u_n\|_{L^1} \leqslant \bar{\beta} + e^{-\mu_0 n} \|u_0\|_{L^1}, \tag{23}$$

with $\bar{\beta} = \beta/(1 - e^{-\mu_0})$. By the second equation of (22), we have

$$\|c_1\|_{L^1} \leqslant a\|c_0\|_{L^1} + a\|u_0\|_{L^1},$$

with $a = pe^{-\mu_0} < 1$. It then follows that

$$\begin{aligned}
\|c_n\|_{L^1} &\leqslant a\|c_{n-1}\|_{L^1} + a\|u_{n-1}\|_{L^1} \\
&\leqslant a(\|c_{n-2}\|_{L^1} + a\|u_{n-2}\|_{L^1}) + a\|u_{n-1}\|_{L^1} \\
&\leqslant a^n\|c_0\|_{L^1} + (a^n\|u_0\|_{L^1} + a^{n-1}\|u_1\|_{L^1} + \cdots + a\|u_{n-1}\|_{L^1}) \\
&\leqslant a^n\|c_0\|_{L^1} + (a^n\|u_0\|_{L^1} + a^{n-1}(\bar{\beta} + e^{-\mu_0}\|u_0\|_{L^1}) \\
&\qquad + \cdots + a(\bar{\beta} + e^{-\mu_0(n-1)}\|u_0\|_{L^1})) \\
&\leqslant a^n\|c_0\|_{L^1} + \frac{\bar{\beta}a}{1-a} + ne^{-\mu_0 n}\|u_0\|_{L^1}. \quad\quad (24)
\end{aligned}$$

By (23)-(24), S is point dissipative and the orbits of bounded sets are bounded.

To see S is α-condensing, we decompose S as $S = S_1 + S_2$, where

$$S_1(u_0, c_0) = \mathcal{G}(\tau, x, y)(B + (1 - q)\, U(1^-), (1 - q)pC(1^-))$$

and

$$S_2(u_0, c_0) = (qu(1^-, x, y), qpc(1^-, x, y)).$$

Since S_1 is of rank 1, it is compact. By (19),

$$\|S_2(u_0, c_0)\|_{L^1} \leqslant qe^{-\mu_0}(\|u_0\|_{L^1} + \|c_0\|_{L^1}).$$

Therefore, for any bounded set $B \subset Y$,

$$\boldsymbol{\alpha}(S(B)) = \boldsymbol{\alpha}(S_2(B)) \leqslant qe^{-\mu_0}\boldsymbol{\alpha}(B).$$

Thus, S is $\boldsymbol{\alpha}$-condensing. Since S is point dissipative, $\boldsymbol{\alpha}$-condensing, and the orbits of bounded sets of S are bounded, S has a global attractor.

5 Numerical simulations

In this section, we provide numerical simulations. The parameters used in the simulations are listed in Table 1 below. We note that $\overline{U}_+$ and $\overline{U}_-$ are the equilibria (for the total population) of the model without contamination, where their formulas are given in Section 3.1. Forager bees are approximately 25% of bees in a colony ([1]). The number of bees in a colony may vary from $20,000$ to $60,000$ ([7]) and in the simulations we choose $\overline{U}_+ = 10,000$ as a typical value for a stabilized colony. We choose $\overline{U}_- = 7,000$ as a typical value for the viable population size threshold. We use the values of $\overline{U}_+$, $\overline{U}_-$, and the forager mortality parameter μ to estimate β and χ, as in Section 3.1.

Forager bees have a range of several kilometers ([1], [28], [50]). In the simulations, we use a rectangular domain of 2 km by 2 km, which is represented as $[0, 2] \times [0, 2]$. We suppose that the hive is at the center $(1, 1)$ of the foraging domain. We assume that forager bees mostly remain removed from
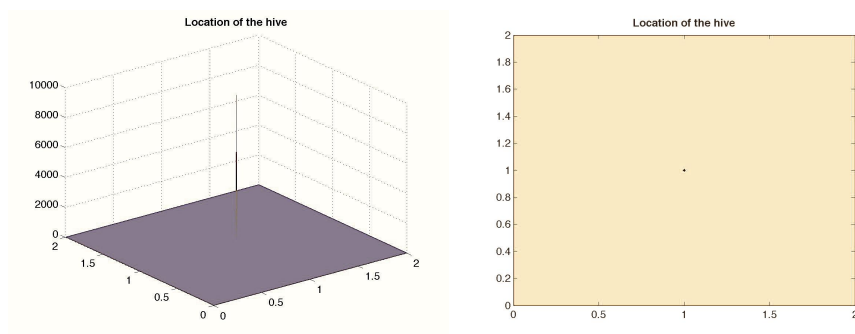
the boundaries of this region. We set the initial distribution at the hive as $u_0(x,y) = N_0 \mathcal{G}(x,y)$, where $N_0 = 10,000$ and $\mathcal{G}(x,y)$ is a Gaussian density function centered at $(1,1)$ with standard deviation $1.5812\ 10^{-4}$. The initial value $u_0(x,y)$ is shown in Figure 1. We interpret a day to be the time of sunlight between successive calendar days, which allows seasonal and regional variability in the time variable t in days. The spatially dependent contamination rate $\alpha(x,y)$ is shown in Figure 2. We set $\alpha(x,y) = \alpha_0(\mathcal{G}_1(x,y) + \mathcal{G}_2(x,y))$, where $\alpha_0 = 0.5$ and $\mathcal{G}_1(x,y)$ (respectively $\mathcal{G}_2(x,y)$) is a Gaussian distribution function centered at $(0.55, 0.55)$ (respectively $(1.45, 1.45)$) with standard deviation 0.1. This means the contamination due to pesticide in the environment is concentrated around the two locations centered at $(0.55, 0.55)$ and $(1.45, 1.45)$.

The parameter p has the following interpretation: $1 - p$ is the fraction of contaminated forager bees that have an increased homing failure due to contamination, beyond the normal homing failure of uncontaminated forager bees incorporated into the mortality rate μ. The parameter q is the fraction of forager bees, both contaminated and uncontaminated, that return each day to their previous locations ([8], [29], [55]). We note that the experiments in [30] found that 93% of bees followed individually acquired information to return to their previous spatial locations. In our simulations we will vary both p and q to illustrate the importance of spatial heterogeneity of contaminated regions for CCD.

Parameter	Description	Estimated value - Reference
$\overline{U}_+$	Stable uncontaminated equilibrium population size	$10,000$ [16], [17], [19], [64]
$\overline{U}_-$	Unstable uncontaminated equilibrium population size	$7,000$ [16], [17], [19], [64]
μ	Mortality rate due to homing failure or other causes	$1/6.5$ day^{-1} [5], [6], [17], [23], [33], [47], [62]
β	Maximal production parameter	2421.13 [63]
χ	Sigmoidal Hill production parameter	7173.56 [63]
$1-p$	Homing failure fraction of bees due to contamination	$.7 - .9$ [32], [33]
q	Fraction of bees returning to their previous location each day	$q \in [0,1]$ [29], [30]
ε	Diffusion rate	$0.1\ km^2$ day^{-1} [22], [35], [46], [45], [50]
$\mathcal{G}(x,y)$	Initial Gaussian distribution of bees in the hive	center at $(1.0km, 1.0km)$
σ	Standard deviation of $\mathcal{G}(x,y)$	1.5812×10^{-4}
$\alpha(x,y)$	Spatial contamination rate	$0.5(\mathcal{G}_1(x,y) + \mathcal{G}_2(x,y))$
$\mathcal{G}_1(x,y)$	Gaussian distribution for contaminated region 1	center at $(0.55km, 0.55km)$, standard deviation 0.1
$\mathcal{G}_2(x,y)$	Gaussian distribution for contaminated region 2	center at $(1.45km, 1.45km)$, standard deviation 0.1

Table 1 *This table lists the parameters used in the simulations. β and χ are estimated from $\overline{U}_+$, $\overline{U}_-$, and μ, as in Section 3.1.*

Fig. 1 *The initial distribution $u_0(x,y)$ of forager bees in the hive. The hive is located at the center of a rectangular domain 2 km by 2 km. $u_0(x,y) = N_0 \mathcal{G}(x,y)$, where $N_0 = 10,000$ and $\mathcal{G}(x,y)$ is a Gaussian density function centered at $(1,1)$ with standard deviation 1.5812×10^{-4}. The initial condition in the right figure shows a visible black dot in the center. The left figure shows a narrow pin-like distribution.*

In the simulations, it is assumed that there are no contaminated bees at the beginning of the first day, which corresponds to the insertion of a managed colony into an agricultural setting. The simulations show the spatial change between the first and second days. After the second day, the spatial pattern of contaminated bees is approximately the same in the following days, but with changes in total populations numbers. Thus, we show only the spatial distributions in the first two days in Figures 3, 4, 6, and 7.
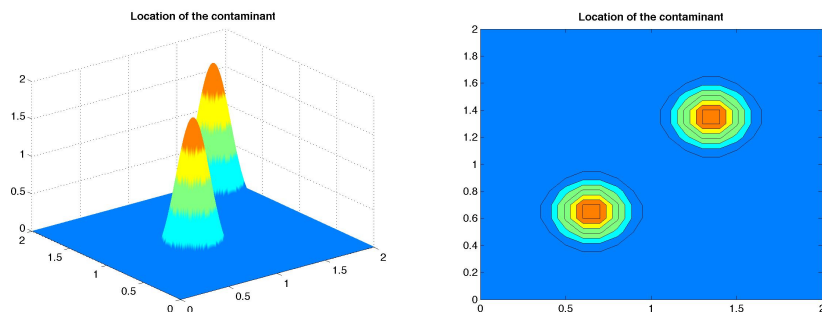
Fig. 2 *These figures show the function $\alpha(x,y) = \alpha_0(\mathcal{G}_1(x,y) + \mathcal{G}_2(x,y))$, which represents the intensity of two contaminated regions in the environment. Here, $\alpha_0 = 0.5$ and $\mathcal{G}_1(x,y)$ (respectively $\mathcal{G}_2(x,y)$) is a normal distribution function centered at $(0.55, 0.55)$ (respectively $(1.45, 1.45)$) with standard deviation 0.1.*

5.1 Simulation with $p = 1.0$ and $q = 0.0$

In the first simulation, we set $p = 1.0$ and $q = 0$, which means that there is no increase in homing failure of contaminated bees above normal homing failure incorporated into μ, and no forager bees remember their locations from the previous day. Figures 3 and 4 show the spatial density of uncontaminated and contaminated bees, respectively. Figure 3 shows that the uncontaminated bees are gradually spreading out from the hive in the first two days, independently of the location of the two contaminated regions. Figure 4 shows that contaminated bees concentrate around the pesticide locations during the first day and gradually spread out randomly from the hive in the second day.

5.2 Simulation with $q = 0.0$ and $p = 1.0$, 0.898, and 0.684

In this simulation, we explore the effect of varying p numerically. We set $q = 0.0$, which means that no bees remember their locations from the previous day. We show three simulations, with $p = 1.0$, 0.898 and 0.684. We see in Figure 5 that the total population remains above $\overline{U}_- = 7,000$ for $p = 1.0$, but not for $p = 0.898$ and p = 0.684. CCD occurs for $p = 0.898$ and p = 0.684, but not for $p = 1.0$. Therefore, the higher homing rate failure of contaminated bees may collapse the colony. In this simulation, $7,000$ is a threshold value for collapse or persistence. The reason is as follows: sum the two equations of (11) to obtain

$$(u + c)(t, \cdot, \cdot) = e^{-\mu t} T(t)(u_0 + c_0), \ t \in (0, 1);$$

integrate in space to obtain

$$U(1^-) + C(1^-) = e^{-\mu}(U(0) + C(0)),$$

and sum (12)-(13) and integrate in space to obtain

$$U(1) + C(1) \leqslant \frac{\beta \ (e^{-\mu}(U(0) + C(0)))^2}{\chi^2 + (e^{-\mu}(U(0) + C(0)))^2} + e^{-\mu}(U(0) + C(0)), \qquad (25)$$

where " $\leqslant$ " becomes " $=$ " if and only if $p = 1.0$. This means that $\overline{U}_- = 7,000$ is a critical value for the total population. That is, if $p = 1.0$, $U(n) + C(n)$ converges to 0 if it is below $7,000$ for some n, and $U(n) + C(n)$ persists if it is above $7,000$ for some n. If $p < 1.0$, by (25), we still have that $U(n) + C(n)$ converges to 0 if it is below $\overline{U}_- = 7,000$ for some n. In Figure 5, the total population of forager bees falls sharply below $7,000$ when $p = 0.898$ or $p = 0.684$, but converges to $\overline{U}_+ = 10,000$ when $p = 1.0$.
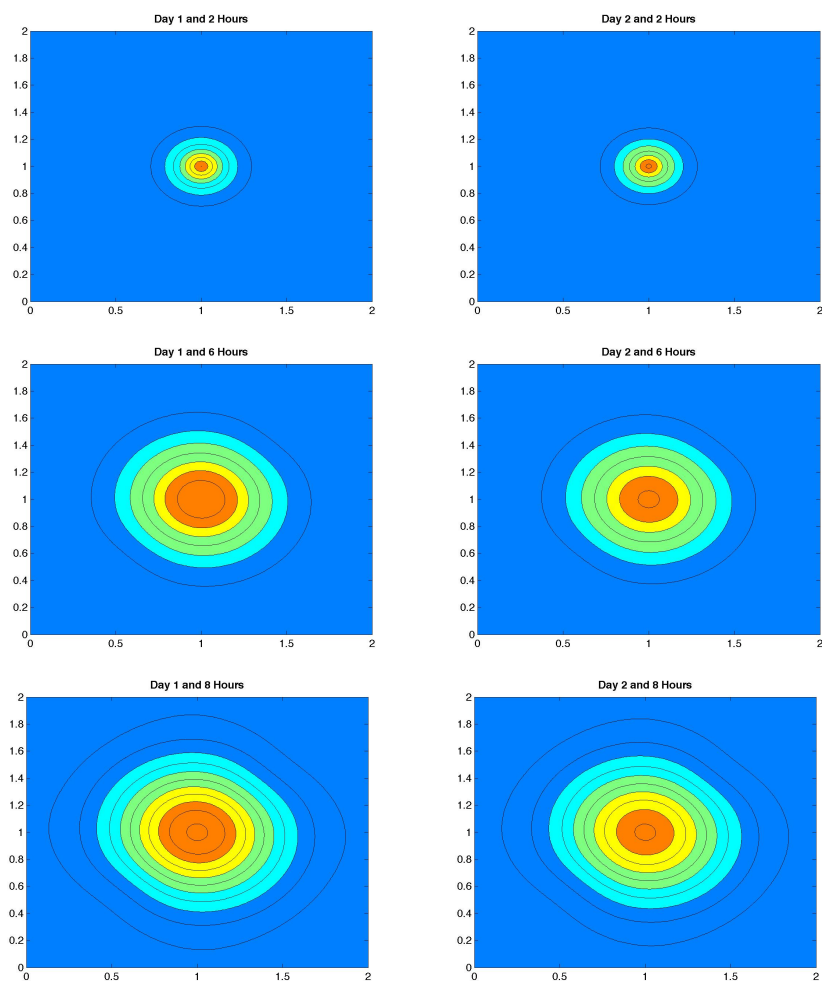
Fig. 3 *These figures show the density of uncontaminated bees at time $t = 2, 6, 8$ hours after the sunrise at day 1 (left side) and day 2 (right side). Here, $p = 1.0$ (there is no increase in homing failure of contaminated bees above normal homing failure) and $q = 0$ (all foraging bees diffuse randomly each day starting from the hive).*

5.3 Simulation with $p = 1.0$ and $q = 0.9$

In this simulation, all contaminated bees return home ($p = 1.0$) and 90% of all bees return to their locations from the previous day ($q = 0.9$). Figure 6 shows that the uncontaminated bees are asymmetrically spreading from the hive on the second day, compared with Figure 3, when $q = 0$. Figure 7 shows that the contaminated bees arise from the two contaminated regions in the first day, which is similar to Figure 4. However, in the second day, the contaminated bees
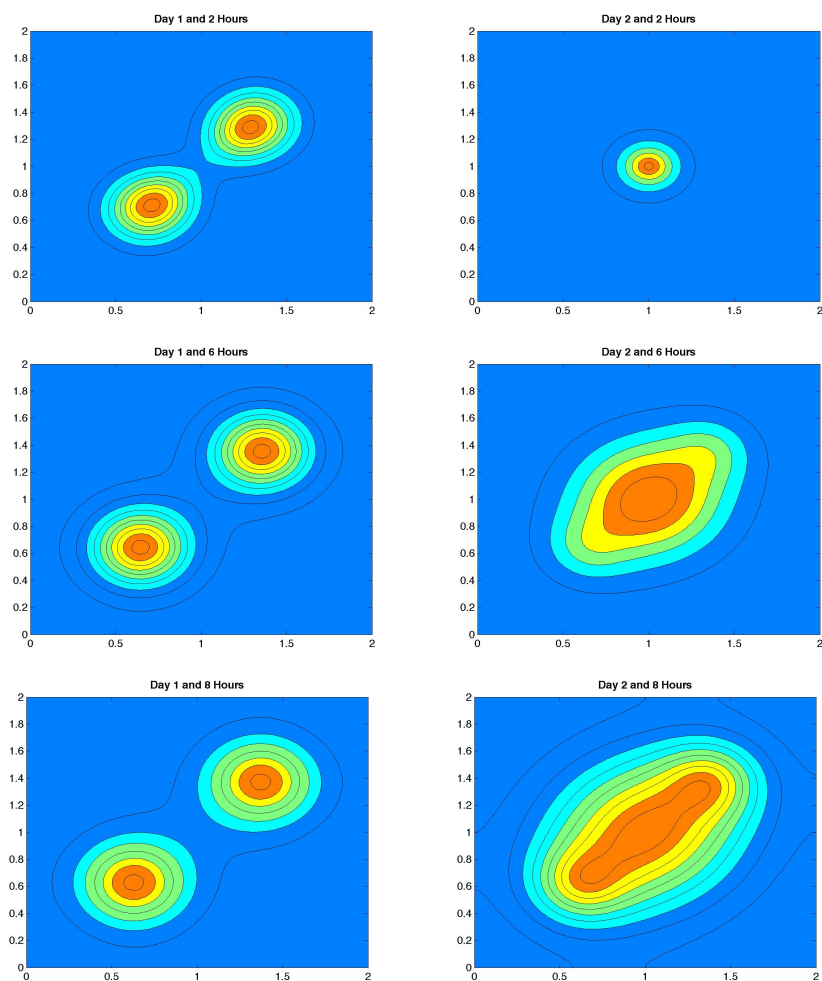
Fig. 4 *These figures show the density of contaminated bees at time $t = 2, 6, 8$ hours after the sunrise at day 1 (left side) and day 2 (right side). As in Figure 3, $p = 1.0$ (there is no increase in homing failure of contaminated bees above normal homing failure incorporated) and $q = 0.0$ (all foraging bees diffuse randomly each day starting from the hive).*

are concentrating near the two contaminated regions, which is in contrast to the second day in Figure 4.

5.4 Simulation with $q = 0.9$ and $p = 1.0$, 0.898, and 0.684

In this simulation, we assume $q = 0.9$ (90% of bees return to their location from the previous day). Figure 8 shows three simulations with $p = 1.0$, 0.898, and 0.684. We observe that the total number of uncontaminated bees decreases
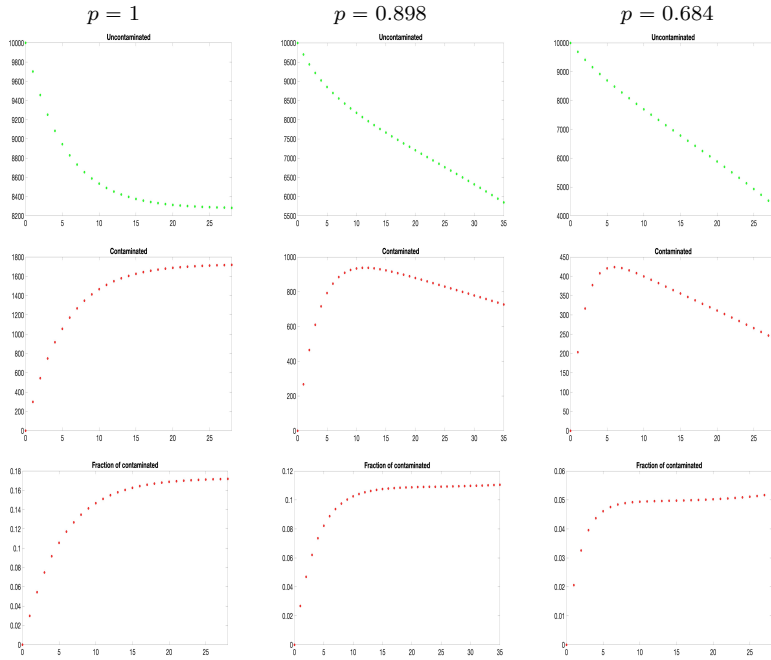
Fig. 5 *The fraction $q = 0.0$ and the fraction p is 1.0 (left), 0.898 (middle) and 0.684 (right). The first row of figures show the total number of uncontaminated bees, the second row of figures show the total number of contaminated bees, and the last row of figures show the fraction of contaminated bees over the total number of bees. CCD occurs for $p = 0.898$ and $p = 0.684$, but not for $p = 1.0$. The horizontal axis variable is days.*

in each case, and the total number of bees, both contaminated and uncontaminated, falls sharply for $p = 0.898$ and $p = 0.684$, but stabilizes for $p = 1.0$. CCD occurs for $p = 0.898$ and p = 0.684, but not for $p = 1.0$.

In Figure 9, we show the same simulations as in Figure 8, except that $q = 0.1$ (10% of bees return to their location from the previous day). Compared to Figure 8, the number of contaminated bees rises more quickly when $q = 0.9$ than when $q = 0.1$. The reason is, when uncontaminated bees return repeatedly to contaminated locations remembered from previous days, they are more likely to become contaminated from these multiple visits. This feature depends on the level of the contamination rate $\alpha(x, y)$, which in this example, requires multiple visits to a contaminated region for a forager bee to become contaminated.

In Figure 10, we show that for the same value of $p = 0.9 < 1$, CCD occurs for $q = 0.9, 0.5, 0.1$. Actually, the total population of bees for $q = 0.9, 0.5$ falls below 7000 at day 28, and therefore CCD occurs. When $q = 0.1$, it is not clear from the figure whether CCD occurs. However, if we run the simulation with more iterations, one can see that CCD occurs eventually. Therefore, the contaminated population rises and the total population falls more quickly and CCD is more likely to occur when q is larger. We remark that it is possible to
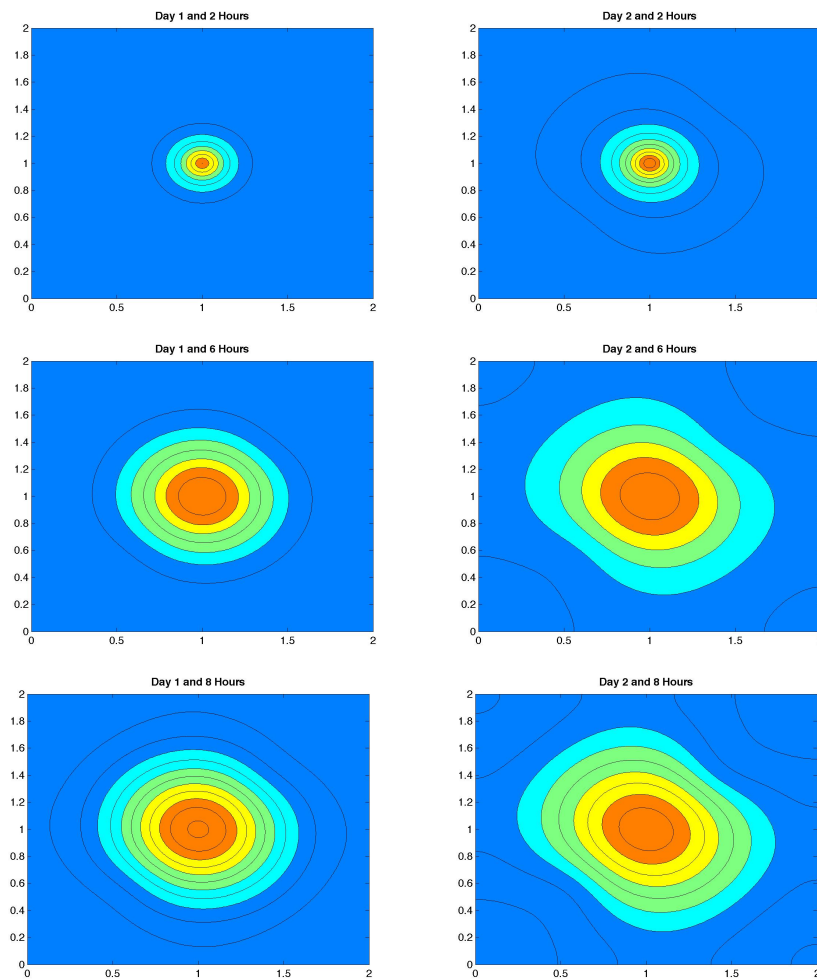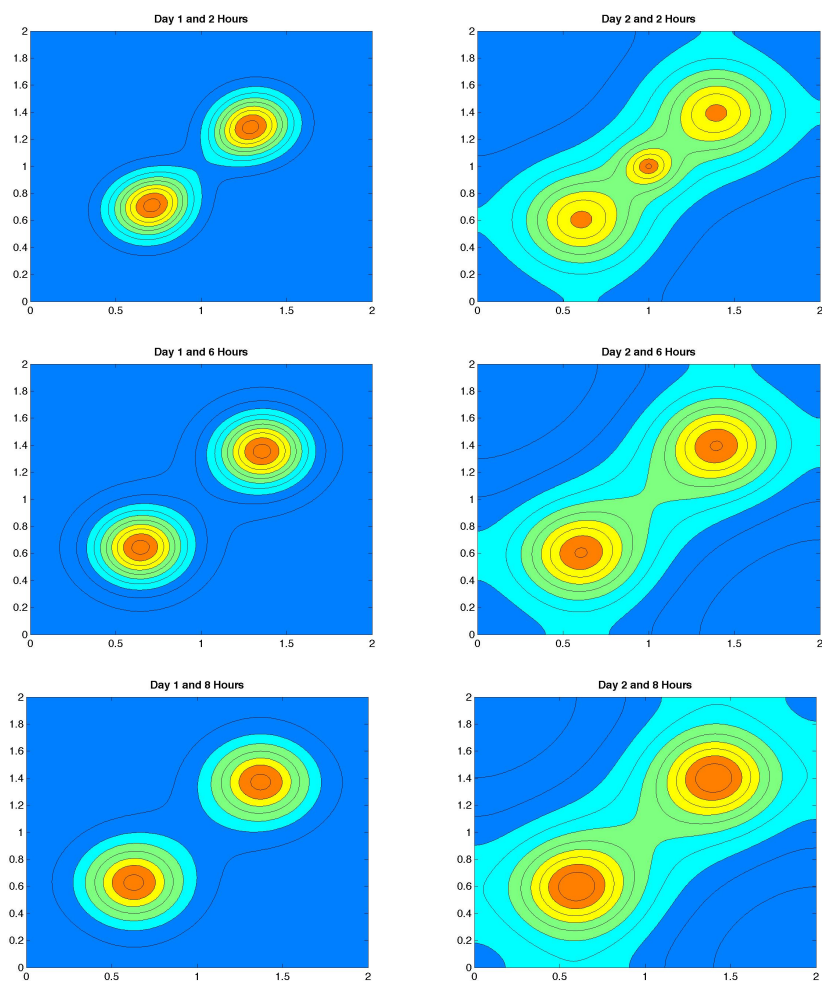
Fig. 6 *These figures show the density of uncontaminated bees at time $t = 2, 6, 8$ hours after the sunrise at day 1 (left side) and day 2 (right side). Here, $p = 1.0$ (all contaminated bees return home) and $q = 0.9$ (90% bees go straight to locations from the previous day).*

find a value for p that is close to 1 (e.g. $p = 0.99$) such that CCD occurs when q is close to 1 and CCD is avoided when q is close to 0. However, with our current parameter values, it requires enormous amount of iterations to confirm whether the total population converges to zero and a positive equilibrium.

6 Conclusions

We have analyzed the impact of spatially heterogeneous environmental pesticide contamination (EPC) as a cause of honey bee colony collapse disorder

Fig. 7 *These figures show the density of contaminated bees at time $t = 2, 6, 8$ hours after the sunrise at day 1 (left side) and day 2 (right side). Here, $p = 1.0$ (all contaminated bees return home) and $q = 0.9$ (90% of bees go straight to locations from the previous day).*

(CCD). We have focused on spatial foraging patterns of foraging honey bees and spatial variation in the locations of pesticide contamination. Foraging honey bees depart and return to their colony hive each day, and we have incorporated this behavior into the equations of our model. Many studies of honey bee foraging have reported the ability of foraging bees to return to previous locations in successive days, and we have incorporated this behavior into our model. This navigation capacity arises from individually acquired information.

Our model consists of equations for the spatial distributions of uncontaminated and contaminated forager bees. Our model has three key features:
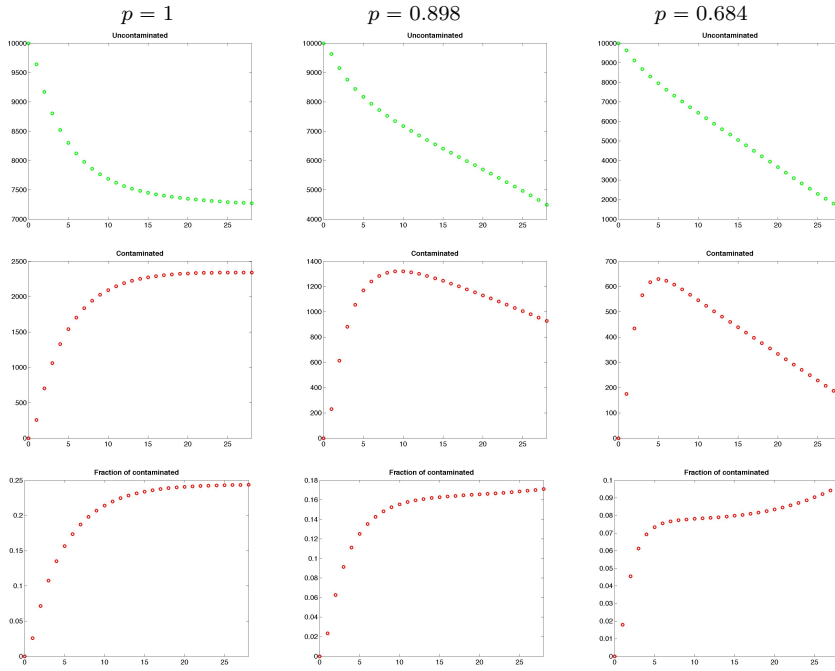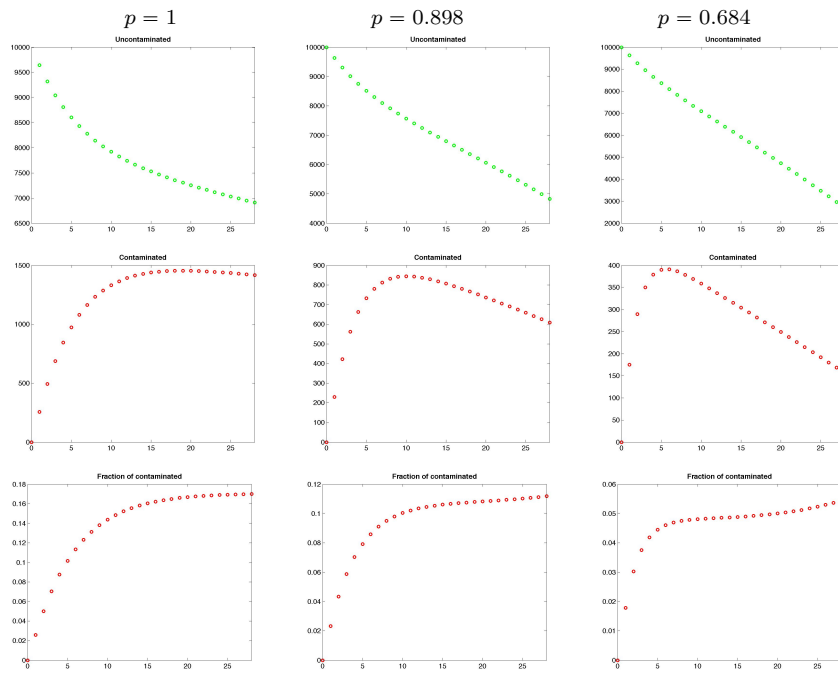
Fig. 8 *The fraction $q = 0.9$ and the fraction p is 1.0 (left), 0.898 (middle) and 0.684 (right). The first row of figures show the total number of uncontaminated bees, the second row of figures show the total number of contaminated bees, and the last row of figures show the fraction of contaminated bees over the total number of bees. CCD occurs for $p = 0.898$ and $p = 0.684$, but not for $p = 1.0$. The horizontal axis variable is days.*

1. Honey bee colonies have a population viability threshold, below which CCD occurs. In our model this threshold is connected to a parameter p that represents the fraction of contaminated forager bees that maintain their ability to return home each day. If the total population of forager bees, both contaminated and uncontaminated, remains above this viability threshold, then CCD is avoided.

2. The fraction q of forager bees that return each day to their previous locations affects the proportion of forager bees that becomes contaminated. If spatial variation is present in the contaminated environment and q is relatively high, then a higher proportion of forager bees become contaminated, because the probability of contamination is increased with repeated visits to the same contaminated site.

3. CCD is quantifiable in terms of the parameters p and q, with each parameter contributing its effect to the outcome.

Our model is relevant for managed honey bee colonies in industrial agriculture, where environmental pesticide exposure is a world-wide problem. In these settings, CCD can be reduced by the following measures: (1) reduction of pesticide use in regions where managed colonies are located; (2) identification

Fig. 9 *The fraction $q = 0.1$ and the fraction p is 1.0 (left), 0.898 (middle) and 0.684 (right). The first row of figures show the total number of uncontaminated bees, the second row of figures show the total number of contaminated bees, and the last row of figures show the fraction of contaminated bees over the total number of bees. CCD occurs for $p = 0.898$ and $p = 0.684$, but not for $p = 1.0$. The horizontal axis variable is days.*

of pesticide-contaminated regions and placement of managed colonies to avoid these regions; (3) maintenance of managed colonies at higher population levels that remain above population viability thresholds.
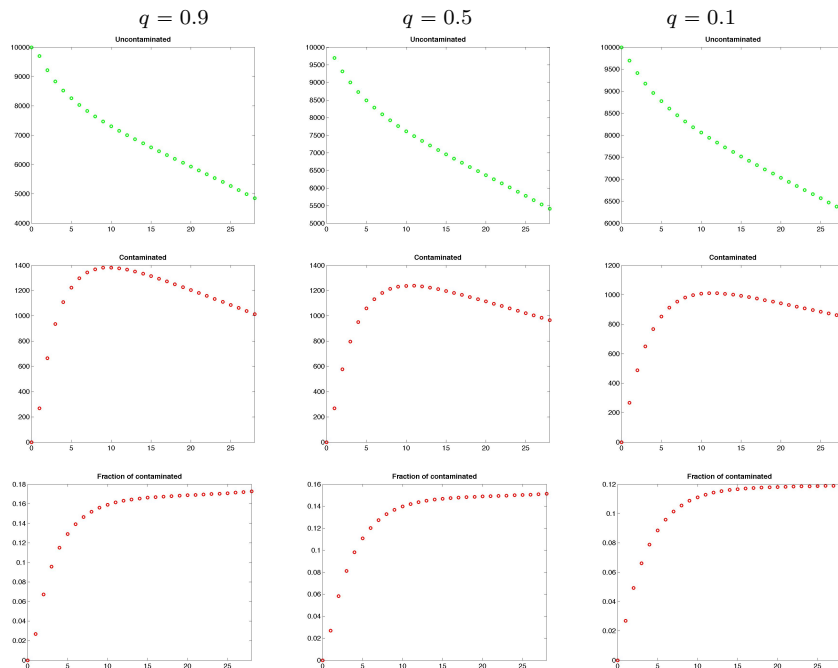
Fig. 10 *The fraction $p = 0.9$ and the fraction q is 0.9 (left), 0.5 (middle) and 0.1 (right). The first row of figures show the total number of uncontaminated bees, the second row of figures show the total number of contaminated bees, and the last row of figures show the fraction of contaminated bees over the total number of bees. Although CCD occurs for all three cases, the total population drops more quickly when q is larger.* The horizontal axis variable is days.

References

1. H. F. Abou-Shaara, The foraging behaviour of honey bees, *Apis mellifera*: a review, *Veterinarni medicina*, **59(1)**, 1-10 (2014).
2. H.T. Banks, J. E. Banks, R. Bommarco, *et al.*, Modeling bumble bee population dynamics with delay differential equations, *Ecological Modelling*, **351**, 14-23 (2017).
3. A. B. Barron, Death of the bee hive: understanding the failure of an insect society, *Science Direct*, **10**, 45-50 (2015).
4. S. Bernardi and E. Venturino, Viral epidemiology of the adult *Apis Mellifera* infested by the Varroa destructor mite, *Science Direct* (2016).
5. M.I. Betti, L. M. Wahl and M. Zamir, Effects of infection on honey bee population dynamics: a model, *PLoS ONE*, **9(10)** (2014).
6. M. Betti, J. LeClair, L. M. Wahl, *et al.*, Bee++: An object-oriented, agent-based simulator for honeybee colonies, *Pop. Sci.*, **8(31)** (2017).
7. C. Binni, How it works: Honeybee society, *Pop. Sci.* April 10, 2013.
8. J. C. Biesmeyer and M. C. W. Ermers, Social foraging in stingless bees: how colonies of *Melipona fasciata* choose among nectar sources, *Behav. Ecol. Sociobiol.* **46** (2005),129-140.
9. T. Blacquiére, G. Smagghe, C. A. M. van Gestel, *et al.*, Neonicotinoids in bees: a review on concentrations, side-effects and risk assessment, *Ecotoxicology*, **21(4)**, 973-992 (2016).
10. R. D. Booten, Y. Iwasa, J.A.R. Marshall, *et al.*, Stress-mediated Allee effects can cause the sudden collapse of honey bee colonies, *J. Theo. Biol.*, **420**, 213-219 (2017).

11. J. Bryden, R. J. Gill, R. A. A. Mitton, *et al.*, Chronic sublethal stress causes bee colony failure, *Ecol. Lett.*, **16**, 1463-1469 (2013).
12. J. E. Cresswell and H. M. Thompson, Comment on "A common pesticide decreases foraging success and survival in honey bees", *Science*, **337**, September 21 (2012).
13. G.C. Cutler and C.D. Scott-Dupree, Exposure to clothianidin seed-treated canola has no long-term impact on honey bees, *J. Econ. Ent.*, **100(3)**, 765-772 (2007).
14. G.C. Cutler, C.D. Scott-Dupree, M. Sultan, *et al.*, A large-scale field study examining effects of exposure to clothianidin seed-treated canola on honey bee colony health, development, and overwintering success, *Peer J.* (2014).
15. G.C. Cutler and C.D. Scott-Dupree, A field study examining the effects of exposure to neonicotinoid seed-treated corn on commercial bumble bee colonies, *Ecotoxicology*, **23(9)**, 1755-1763 (2016).
16. G. DeGrandi-Hoffman, S. A. Roth, G. L. Loper, and E. H. Erickson, BEEPOP: A honeybee population dynamics simulation model, *Ecol. Mod.*, **45**, 133-150 (1989).
17. G. DeGrandi-Hoffman and R. Curry, A mathematical model of Varroa mite (Varroa destructor Anderson and Trueman) and honeybee *Apis mellifera L.* population dynamics, *Int. J. Acarol.*, **30(3)**, 259-274 (2004).
18. A. Dénes and A. I. Ibrahim, Global dynamics of a mathematical model for a honeybee colony infested by virus-carrying Varroa mites, textit J. Appl. Math. Comp., March, (2019).
19. B. Dennis and W.P. Kemp, How hives collapse: Allee effects, ecological resilience, and the honey bee, *PLoS ONE*, **11(2)** (2016).
20. N. Desneux, A. Decourtye, and J. M. Delpuech, The sublethal effects of pesticides on beneficial arthropods, *Ann. Rev. Ent.*, **52**, 81-106 (2007).
21. G.P. Dively, M. S. Embrey, A. Kamel, *et al.*, Assessment of Chronic Sublethal Effects of Imidacloprid on Honey Bee Colony Health, *PLoS One* (2015).
22. R. Dukas and L. Edelstein-Keshet, The spatial distribution of colonial food provisioners, *J. Theor. Biol.*, **190**, 121-134 (1998).
23. R. Dukas, Mortality rates of honey bees in the wild, *Insectes Sociaux*, **55(3)**, 252-255 (2008).
24. European Food Safety Authority, Neonicotinoids: risks to bees confirmed (2018), *doi* : $10.2903/sp.efsa.2018.EN - 1378$.
25. European Food Safety Authority, Evaluation of the data on clothianidin, imidacloprid and thiamethoxam for the updated risk assessment to bees for seed treatments and granules in the EU (2018), *doi* : $10.2903/sp.efsa.2018.EN - 1378$.
26. G. Gabbriellini, Seasonal effects on honey bee population dynamics: a nonautonomous system of difference equations, *Int. J. Dif. Equ.*, **12(2)**, 211-233 (2017).
27. D. Goulson, E. Nicholls, C. Botas, and E. L. Rotheray, Bee declines driven by combined stress from parasites, pesticides, and lack of flowers, *Science*, **347**, (2015).
28. S. S. Greenleaf, N. M. Williams, R. Winfree, and C. Kremen, Bee foraging ranges and their relationship to body size, *Oecol.*, **153(3)**, 589-596 (2007).
29. C. Grüter and W. M. Farina, The honeybee waggle dance: can we follow the steps? *Trends in Ecology and Evolution*, **24(5)** (2009), 242-247.
30. C. Grüter, M. Sol Balbuena, and W. M. Farina, Informational conflicts created by the waggle dance, *Proc. Roy. Soc. B: Biol.Sci.*, **275** (2008), 1321-1327.
31. J. K. Hale, *Asymptotic Behavior of Dissipative Systems*, Mathematical Surveys and Monographs 25, Amer. Math. Soc., Providence, RI, (1988).
32. M. Henry, M. Béguin, F. Requier, *et al.*, A common pesticide decreases foraging success and survival in honey bees, *Science*, **336(6079)**, 348-350 (2012).
33. M. Henry, N. Cerrutti, P. Aupinel, *et al.*, Reconciling laboratory and field assessments of neonicotinoid toxicity to honeybees, *Proc. R. Soc. B*, **282** (2015).
34. Z. Y. Huang and G. E. Robinson, Regulation of honey bee division of labor by colony age demography, *Behavioral Ecol. Social.*, **39**, 147-158 (1974).
35. D. T. Iles, N. M. Williams, and E. E. Crone, Source-sink dynamics of bumblebees in rapidly changing landscapes, *J. Appl. Ecol.*, **55**, 2802-2811 (2018).
36. Y. Kang and G. Theraulaz, Dynamical models of task organization in social insect colonies, *Bull. Math. Biol.*, **78(5)**, 879-915 (2016).

37. Y. Kang, K. Blanco, T. Davis, Y. Wang and G. DeGrandi-Hoffman, Disease dynamics of honeybees with Varroa destructor as parasite and virus vector, *Math. Biosci.*, **275**, 71-92 (2016).

38. L. G. Kawaguchi, O. Kazuharu, and T. Yukihiko, Contrasting responses of bumble bees to feeding conspecifics on their familiar and unfamiliar flowers, *Proc. Roy. Soc. B*, **39(1626**, (2007).

39. D.S. Khoury, M.R. Myerscough, and A.B. Barron, A quantitative model of honey bee colony population dynamics, *PLoS ONE*, **6(4)** (2011).

40. C.M. Kribs-Zaleta and C. Mitchell, Modeling colony collapse disorder in honeybees as a contagion, *Math. Biosci. Eng.*, **11(6)**, 1275-1294 (2014).

41. E. Leadbeater and L. Chittka, Bumble-bees learn the value of social cues through experience, *Biol. Lett.*, **5** (2009).

42. I. Leoncini, Y. Le Conte , G. Costagliola, *et al.*, Regulation of behavioral maturation by a primer pheromone produced by adult worker honey bees, *Proc. Nat. Acad. Sci.*, **101**, 17559-17564 (2004).

43. M. B. Lerata, J. M-S. Lubuma, and A. A. Yusuf, Continuous and discrete dynamical systems for the declines of honeybee colonies, *Math. Meth. Appl. Sci.*, **41(18)**, 8724-8740 (2018).

44. W. G. Meikle, J. J. Adamczyk, M. Weiss, *et al.*, Sublethal effects of imidacloprid on honey bee colony growth and activity at three sites in the U.S. *PLoS ONE* (2016).

45. A. Mogilner and L. Edelstein-Keshet, A non-local model for a swarm, *J. Math. Biol.*, **38** (1999), 534-570.

46. K. Messan, G. Degrandi-Hoffman, C. Castillo-Chavez, and Y. Kang, Migration Effects on Population Dynamics of the Honeybee-mite Interactions, *Math. Mod. Nat. Phen.*, **12(2)**, 84-115 (2017).

47. M. R. Myerscough, D. S. Khoury, S. Ronzani, and A. B. Barron, Why do hives die? Using mathematics to solve the problem of honey bee colony collapse, In: Anderssen B. *et al.* (eds) *The Role and Importance of Mathematics in Innovation. Mathematics for Industry*, **25**, Springer, Singapore (2017).

48. P. Magal, G. F. Webb, and Y. Wu, An Environmental Model of Honey Bee Colony Collapse Due to Pesticide Contamination, *Bull. Math. Bio.*, **81(12)**, 4908-4931 (2019).

49. B. K. Nguyen, C. Saegerman, C. Picard, *et al.*, Does imidacloprid seed-treated maize have an impact on honey bee mortality?, *J. Econ. Ent.*, **102(2)**, 616-623 (2009).

50. J. L. Osborne, S. J. Clark, R. J. Morris, *et al.*, A landscape-scale study of bumble bee foraging range and constancy, using harmonic radar, *J. Appl. Ecol.*, **36**, 519-533 (1999).

51. E. Pilling, E. Cambell, M. Coulson, *et al.*, A four-year field program investigating long-term effects of repeated exposure of honey bee colonies to flowering crops treated with thiamethoxam, *PLoS ONE* (2013).

52. V. Ratti, P.G. Kevan, and H.J. Eberl, A mathematical model for population dynamics in honeybee colonies infested with Varroa destructor and the acute bee paralysis virus, *Can. Appl. Math. Q.*, **21(1)**, 63-93 (2013).

53. V. Ratti, P. G. Kevan and H. J. Eberl, A mathematical model of forager loss in honeybee colonies infested with Varroa destructor and the acute bee paralysis virus, *Bull. Math. Biol.*, **79(6)**, 1218-1253 (2017).

54. L. A. Richardson, A swarm of bee research, *PLos Biol.*, January 9, 2017.

55. J. R. Riley, U. Greggers, A. D. Smith, *et al.*, The flight paths of honeybees recruited by the waggle dance, *Nature*, **435** (2005):205.

56. D. Rolke, S. Fuchs, B. Grunewald, *et al.*, Large-scale monitoring of effects of clothianidin-dressed oilseed rape seeds on pollinating insects in Northern Germany: effects on honey bees (*Apis mellifera*), *Ecotoxicology*, **25(9)**, 1648-1665 (2016).

57. M. Rundlof, G. K. S. Andersson, R. Bommarco, *et al.*, Seed coating with a neonicotinoid insecticide negatively affects wild bees, *Nature*, **521**, 77-80 (2015).

58. C. Sandrock, L. G. Tanadini, J. S. Pettis, *et al.*, Sublethal neonicotinoid insecticide exposure reduces solitary bee reproductive success, *Agri. For. Ent.* **16**, 119-128 (2014).

59. C. W. Schneider, J. Tautz, B. Grünewald, *et al.*, RFID tracking of sublethal effects of two neonicotinoid insecticides on the foraging behavior of *Apis mellifera*, *PLoS ONE* **7(1)**, (2012).

60. D. A. Stanley, A. L. Russell, S. J. Morrison, *et al.*, Investigating the impacts of field-realistic exposure to a neonicotinoid pesticide on bumblebee foraging, homing ability and colony growth, *J. Appl. Ecol.* **53**, 1440-1449 (2016).

61. J. D. Thomson, S. Montgomery, and B. A. Thomson, Trapline foraging by bumble bees: II. Definition and detection from sequence data, *Beh. Ecol.* **8(2)** , 199-210 (1997).

62. D. J. Torres, U. M. Ricoy, and S. Roybal, Modeling honey bee populations, *PLoS ONE*, **10(7)** (2015).

63. L. L. Truitt, S. H. McArt, A. H. Vaughn, and S. P. Ellner, Trait-based modeling of multihost pathogen transmission: plant-pollinator networks, *Am. Nat.*, **193(6)**, E149-E167 (2019).

64. D. vanEngelsdorp, J. D. Evans, C. Saegerman, *et al.*, Colony collapse disorder: A descriptive study, *PLoS ONE* **4(8)**, e6481 (2009).

65. K. von Frisch, The Dance Language and Orientation of Bees, Harvard University Press, Cambridge, Massachusetts, 1967.

66. X. Zhao, *Dynamical Systems in Population Biology, 2nd edition*, Springer, New York, 2017.